Chapter 4

Failure Analysis of High Pressure High Temperature Super-Heater Outlet Header Tube in Heat Recovery Steam Generator

Ainul Akmar Mokhtar and
Muhammad Kamil Kamarul Bahrin

Additional information is available at the end of the chapter

http://dx.doi.org/10.5772/intechopen.72116

Abstract

Heat Recovery Seam Generator (HRSG) tube failure is one of the most frequent causes of power plant forced outage. In one of the local power plants, one of the boilers has experienced several defects and failures after running approximately 85,000 hours. 17 tube failures were found at the High Pressure High Temperature Superheater (HPHTSH) outlet header. The aim of this study is to find the root cause of the tube failures and to suggest the remedial action to prevent repetitive failure event. Several analysis methods were conducted to ascertain the potential cause(s) of failure. The results showed that the tubes failed due to long-term creep and thermal fatigue based on the cracking behaviour. Furthermore, the power plant has been operating as a peaking plant which concluded that the tubes have undergone the thermal stress due to frequent temperature change in the tubes. Flow correcting device (FCD) was also found damaged, causing flow imbalance in the tubes. Flow imbalance accelerated the creep degradation on the tubes. It was recommended that the FCD has to be repaired and improved to balance the flow. Furthermore, the extensive life assessment was recommended to be done on all the tubes to avoid future tube failures.

Keywords: boiler tube failure, HRSG, failure analysis

1. Background of study

After nearly 85,000 running hours, one of the boilers, also known as heat recovery steam generator (HRSG), in one of the local power plants has been experiencing 17 boiler tube failures. The power plant was designed as base load plant; however, after 7 years of operation, the plant started changing its operating regime from base load to cyclic load with more

start-up/shutdown. The frequency of tube failures has increased when the plant was having more cyclic operation as compared to 5 years after commissioning. The connecting tubes of the outlet header of HRSG High Pressure High Temperature Superheater (HPHTSH) have suffered leakage, and all the failed tubes were located next to each other in a row (i.e. Row 3) as shown in **Figure 1**.

During the incident, a significant drop of the water level and water pressure was detected at the high pressure (HP) boiler drum due to the extensive leak of these HPHTSH connecting tubes. Then, the plant decided to declare force outage in order for inspection team to carry out proper, thorough inspections to identify the cause of water loss. The suspected tubes of High Temperature Reheat (HTRH), HPHTSH and High Pressure Low Temperature Superheater (HPLTSH) inlet and outlet header were inspected.

The outcomes from the inspection showed that no defects were found on HTRH and HPLTSH inlet and outlet header; however, circumferential cracks were found at 17 tubes on HPHTSH outlet header. The flow correcting devices (FCD) also were found detached and misaligned from its original position. Maintenance team has appointed internal inspection team to investigate the possible failure mechanism and the root cause of HPHTSH outlet header tube failures. Also, they requested external laboratory to conduct a remaining creep life prediction [1].

The main objectives are:

1. To determine metallurgical characteristics and mechanical properties of the failed tube specimens.
2. To identify the root cause of failures and its mechanisms.
3. To provide recommendations for rectification actions in future prevention of the tube failures.

The investigation covered the failure of Tube 8, Tube 9, Tube 10 and Tube 18 of the HPHTSH section. **Figure 2** shows the samples of tube failures. Several analysis methods were carried out to ascertain the potential cause(s) of failure such as visual examination, dimensional

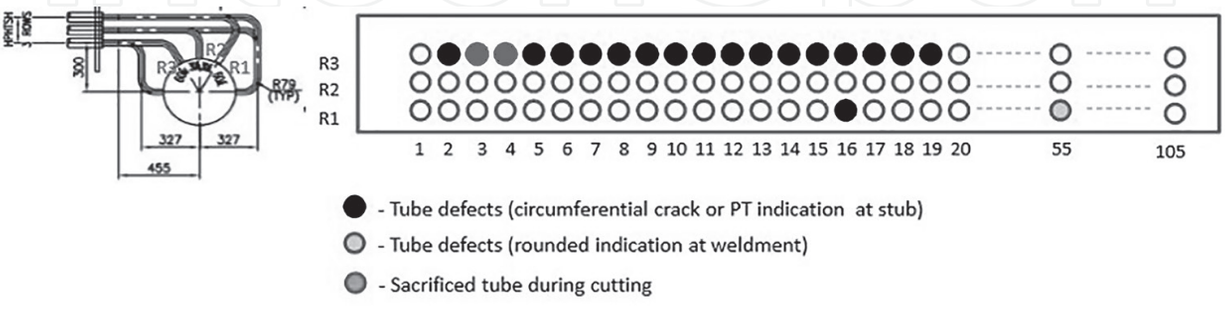

Figure 1. Tube mapping of recent failure of HPHTSH outlet header tubes.

http://dx.doi.org/10.5772/intechopen.72116

Figure 2. Appearance of Row 3 tube failures, (a) Tube 8 and (b) Tube 9.

Type of analysis	Tube 8	Tube 9	Tube 10	Tube 18
Visual inspection	√	√	√	√
Dimensional measurement	√			√
Metallographic examination	√			√
Hardness testing	√			√
XRF analysis	√	√	√	√
Oxide thickness assessment	√			√

Table 1. Analysis done on each tube.

measurement, metallurgical analysis, hardness testing, chemical analysis or X-ray fluorescence (XRF) analysis, oxide layer measurement and creep assessment. Each method of analysis may not cover all tubes due to limited resources and time. **Table 1** shows the analysis method done on those selected tubes.

2. Procedure for HRSG tube failure analysis

Detail visual examination is the first step to determine earlier condition of failed tube. After received the sample, the condition on fireside and waterside surface shall be thoroughly inspected for any abnormal indication and the findings shall be recorded with photographic documentation. Any change of colour, deposit texture, fracture surface, location of defect and morphology should be focussed and recorded.

The next step in the tube failure analysis is to conduct a dimensional analysis. The design data and drawing should be available before proceeding this step. Quantitative assessment on

failed tube with the Vernier calliper or ID/OD micrometre useful in assessing wall thinning, bulging and any corrosion damage. Ultrasonic thickness machine can be used to measure the oxide thickness of failed area and give the idea how long the failure has already taken place. The extent of oxide formation and/or ductile expansion can provide an idea to determine the primary failure mechanism. For example, thick oxide may indicate that the rupture may be due to overheating.

The appearance and/or orientation of crack can be helpful in determining a failure mechanism. While A soot blower erosion typically causes 'fish mouth' and thick-edged appearance, and thermal commonly results in transverse crack at heat-affected zone (HAZ). Normally, the crack shall be examined closely at HAZ and weldment area. Non-Destructive Test (NDT) such as dye-penetrant testing or magnetic particle testing may be necessary to determine the extent of the crack [2].

The evaluation of water chemistry and boiler operation is necessary to determine the failure mechanism. As an example, poor water chemistry will result in flow accelerated corrosion (FAC) on low pressure section or thicker oxide layer in a superheated section. Excessive oxide layer will result in high metal temperature. This will eventually cause high-temperature oxidation and may lead to exfoliation. Quantitative analysis of the internal tube surface commonly involves the determination of the oxide scale value and deposit thickness. Interpretation of these values can define the role of internal deposits in a failure mechanism. Oxide scale values are also used to determine whether chemical cleaning of boiler tubing is required. Wet chemical analysis is often used to determine the elemental composition. A number of spectrochemical analysis techniques can also be used for the quantitative measurement to determine the material percentage in the failed tube. The result will be compared to ASME, 2015, Section II Part D. In boiler construction, there are several cases where the installation or repair work was done using wrong grade of materials. In any cases, wet chemical analysis comparison of the steel can be used to determine the cause of premature failure.

Hardness measurement can be used to estimate the tensile strength/material hardness. The comparison of failed tube harness to accepted hardness range, and the deterioration of the mechanical properties can be determined due to material creep. The micro-Vickers hardness tester is usually used to obtain the hardness profile along the defective surface including HAZ, weldment, and base metal for any microstructure change on the material.

Metallography is key actions in determining the boiler tube failure mechanism. It is also good in assess the following:

a. whether cracks initiated on a waterside or fireside surface

b. the orientation of crack

c. whether a tube failure resulted from hydrogen embrittlement

d. whether a tube failed from short-term or long-term overheating damage

e. whether cracks were caused by creep damage, thermal fatigue, or stress-corrosion cracking.

http://dx.doi.org/10.5772/intechopen.72116

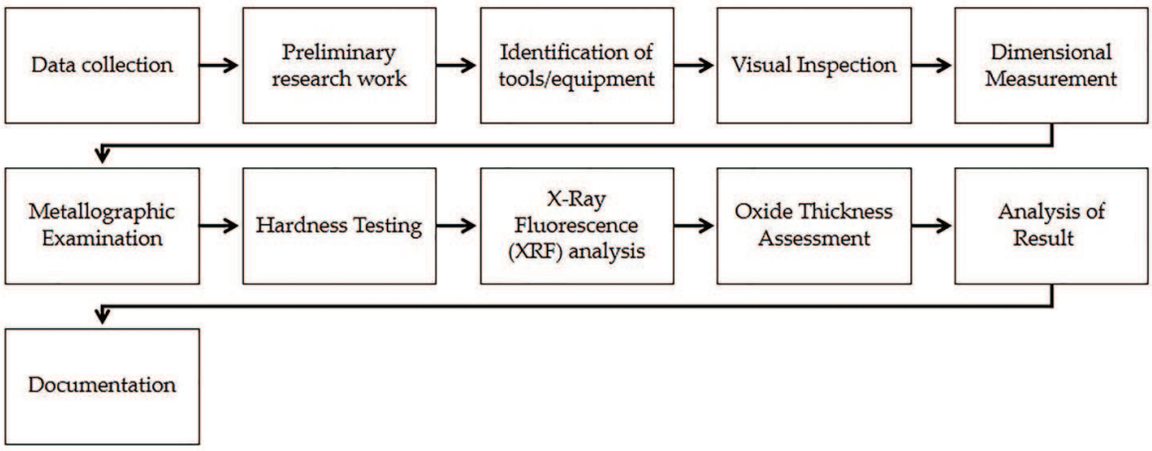

Figure 3. Flow chart of failure analysis activities.

Proper sample orientation and preparation are critical aspects of microstructural analysis. The orientation of the sectioning is determined by the specific failure characteristics of the case. After careful selection, metal specimens are cut with an abrasive cut-off wheel and mounted in a mould with resin or plastic. After mounting, the samples are subjected to a series of grinding and polishing steps. The goal is to obtain a flat, scratch-free surface of metal in the zone of interest. After processing, a suitable etchant is applied to the polished metal surface to reveal microstructural constituents (grain boundaries, distribution and morphology of iron carbides, etc.). **Figure 3** summarizes the failure analysis activities.

3. Results and discussion

3.1. Visual examination

Four tube sections were identified in Row 3 as Tube 8, Tube 9, Tube 10 and Tube 18, and each marked with an arrow indicating the flow direction towards the outlet header. Measurement has showed that the five tube sections have a nominal outer diameter (OD) of 32 mm. All examined tubes comprised bend sections approximately 280 mm long, measured around the extrados of the bend.

The connecting tubes are welded directly on the header without the presence of stubs. Cracks have developed at the heat-affected zone (HAZ) of the welds on the tube side. All cracks were circumferential in nature with no branching characteristics. The cracks propagated at the outer radius plane of the connecting tubes with an average length of approximately 25 mm as shown in **Figure 4**.

The tube sections have not undergone visible bulging and deformation over the entire length. The external surfaces of all sections appeared to be normal, with no signs of significant corrosion/erosion damage. The magnetite layer on the inner, steam-touched surfaces appeared thick, homogenous, adhesive and continuous, with no signs of serious/apparent exfoliation. The circumferential cracks have penetrated the tube wall.

(a) (b)

Figure 4. Appearance of tube failure at Row 3: (a) Tube 8 and (b) Tube 18.

3.2. Dimensional measurement

3.2.1. Thickness measurement

Tube 8 and Tube 18 out of five tubes were chosen for dimensional measurement since the Tube 8 may be a representative of Tube 9 and Tube 10. The tube was cut into six pieces in order to do OD and inner diameter (ID) measurement. The thickness of Tube 8 and Tube 18 was measured by ultrasonic thickness at three locations for each tube, designated as A, B and C. Four spots with respect to clock position 12, 3, 6 and 9 were measured at each location as shown in **Figure 5**. The results are recorded in **Tables 2** and **3**.

The minimum measured thickness readings were compared with the minimum required thickness from the RBI report and Doosan (HRSG OEM) report. Several locations of Tube 8 and Tube 18 showed that the wall thickness was lower than the minimum required thickness, which was considered unsafe and unacceptable. It implied that the risk of stress rupture

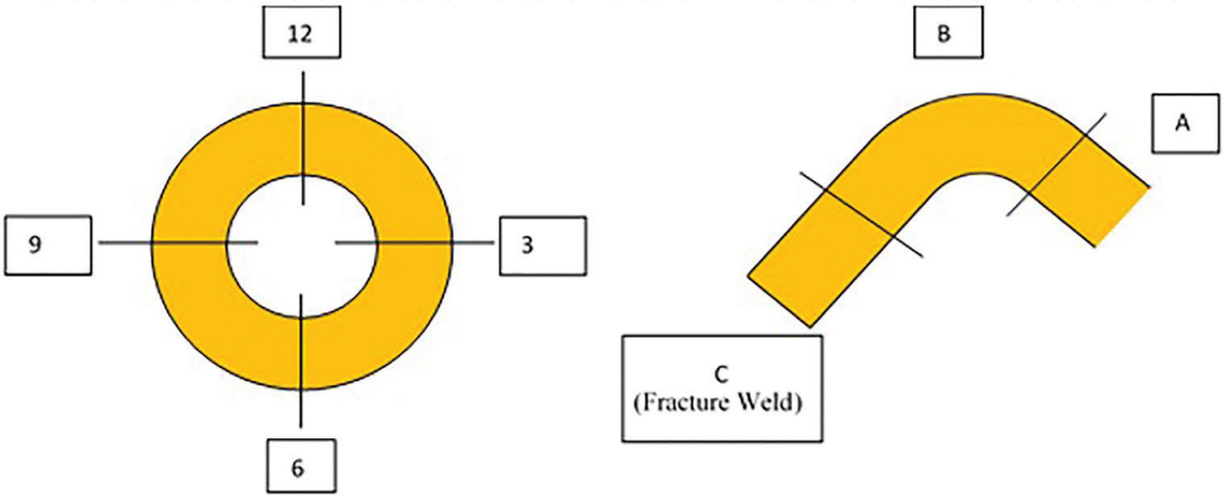

Figure 5. Dimensional references of thickness measurement on a tube.

http://dx.doi.org/10.5772/intechopen.72116

Tube 8				
Location	**12**	**3**	**6**	**9**
A	2.95	2.79	2.86	2.87
	2.96	2.7	2.84	2.83
	2.95	2.76	2.87	2.81
Min value	2.95	2.7	2.84	2.81
B	2.14	2.96	3.28	2.83
	2.16	2.93	3.29	2.89
	2.15	2.95	3.24	2.85
Min value	2.14	2.93	3.24	2.83
C	2.88	2.73	2.83	2.92
	2.81	2.74	2.82	2.9
	2.82	2.73	2.8	2.91
Min value	2.81	2.73	2.8	2.9

Table 2. Thickness reading of Tube 8 (in mm).

was high. The significant wall thinning could be due to the excessive steam oxidation, which caused a high consumption rate of metal.

3.2.2. Outer/inner diameter (OD/ID) measurement

Tube 8 and Tube 18 were cut at an interval length of 50 mm. The sections are designated 1–6 as shown in **Figure 6**. The OD, ID and thickness of each cutting location were measured by Vernier calliper at the area shown in **Figure 7**. The results are recorded in **Tables 4** and **5**.

Tube 18				
Location	**12**	**3**	**6**	**9**
A	2.77	2.63	2.89	2.88
	2.74	2.65	2.91	2.89
	2.75	2.62	2.9	2.83
Min value	2.74	2.62	2.89	2.83
B	2.21	2.86	3.41	2.86
	2.2	2.82	3.43	2.89
	2.19	2.91	3.42	2.81
Min value	2.19	2.82	3.41	2.81
C	2.72	2.72	2.7	2.71
	2.79	2.73	2.78	2.69
	2.74	2.71	2.76	2.72
Min value	2.72	2.71	2.7	2.69

Table 3. Thickness reading of Tube 18 (in mm).

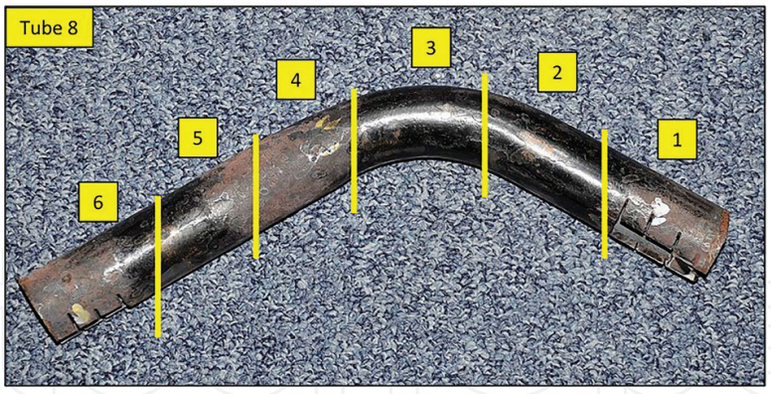

Figure 6. Tube 8 was cut into six sections.

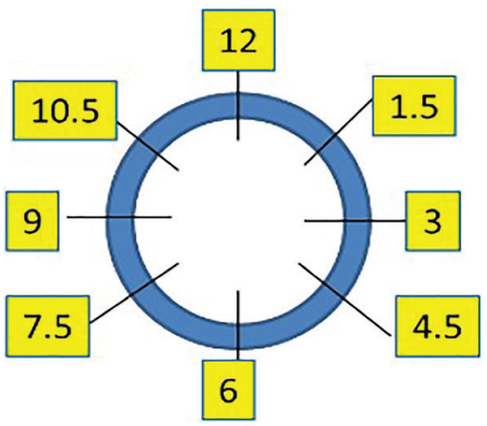

Figure 7. Dimensional reference of OD and ID tube.

The OD and ID for both tubes did not show any significant signs of tube bulging, deformation and wall thinning over the length, as compared to the design values, where OD was 31.8 mm and ID was 26.2 mm.

3.3. Metallographic examination

The metallographic examination was performed on Tube 8 and Tube 18 through the replication method and the standard metallographic preparation method. The replication method was applied on tube surface in a non-destructive manner, while in the standard metallographic method, the cracked part was cut and mounted in cross sections. The damage characteristics of the fractured area in mounted specimens of Tube 8 and Tube 18 are described as follows:

a. The cracks were fairly straight and had a transgranular appearance, thick oxide filled, without branching characteristics. The cracks propagated in the HAZ.

b. Isolated, aligned cavities and microcracks were presented in the vicinity of the cracks. The cavities were predominantly aligned in parallel to the cracks, and some were perpendicular to the cracks.

c. Under high magnifications, the grade 91 microstructure of base metal still appeared normal (martensitic) with no signs of thermal degradation such as phase transformation, grain growth and precipitate coarsening. A small amount of isolated cavities were found in the remote base metal of Tube 8.

d. The fracture surfaces had oxidized heavily. The oxide layers at the steam touch surfaces (inner surface) were considered thick, in excess of 300 μm.

Figure 8 shows the microstructure of Tube 8 at the fracture area at different magnification. Isolated cavities, aligned cavities, microcrack and thick oxidation layer were observed at that particular location.

3.4. Hardness testing

Micro-Vickers hardness was used to measure the mounted specimen hardness of Tube 8 and Tube 18. The applied load for this test was 10 kg load in 5 s. The tested locations include:

a. Heat-affected zone (HAZ)

b. Base metal (near crack's location)

c. Base metal (remote area)

Section	Outer diameter (mm)				Inner diameter (mm)			
	12–6	1.5–7.5	3–9	4.5–10.5	12–6	1.5–7.5	3–9	4.5–10.5
1	31.75	31.89	31.82	31.87	25.25	24.47	25.31	25.31
2	31.90	31.86	31.86	31.87	24.80	24.98	25.22	25.34
3	31.93	30.75	30.65	31.85	25.16	24.11	23.89	24.63
4	31.85	32.03	31.94	31.98	24.63	25.18	25.11	24.84
5	31.88	31.76	31.77	31.87	25.20	25.16	25.55	25.26
6	31.66	31.71	31.60	31.43	25.14	25.11	24.64	24.67

Table 4. OD and ID each section of Tube 8.

Section	Outer diameter (mm)				Inner diameter (mm)			
	12–6	1.5–7.5	3–9	4.5–10.5	12–6	1.5–7.5	3–9	4.5–10.5
1	31.69	31.25	31.57	31.29	25.29	25.12	25.35	25.28
2	31.52	31.74	31.87	30.82	24.84	24.67	25.40	24.17
3	31.31	31.35	30.74	32.22	24.56	23.95	23.84	25.27
4	30.97	30.59	29.51	31.63	24.80	23.78	23.14	25.04
5	32.02	32.31	31.91	32.22	25.18	25.14	25.03	25.33
6	31.86	31.63	31.60	31.60	25.04	24.89	25.35	25.12

Table 5. OD and ID each section of Tube 18.

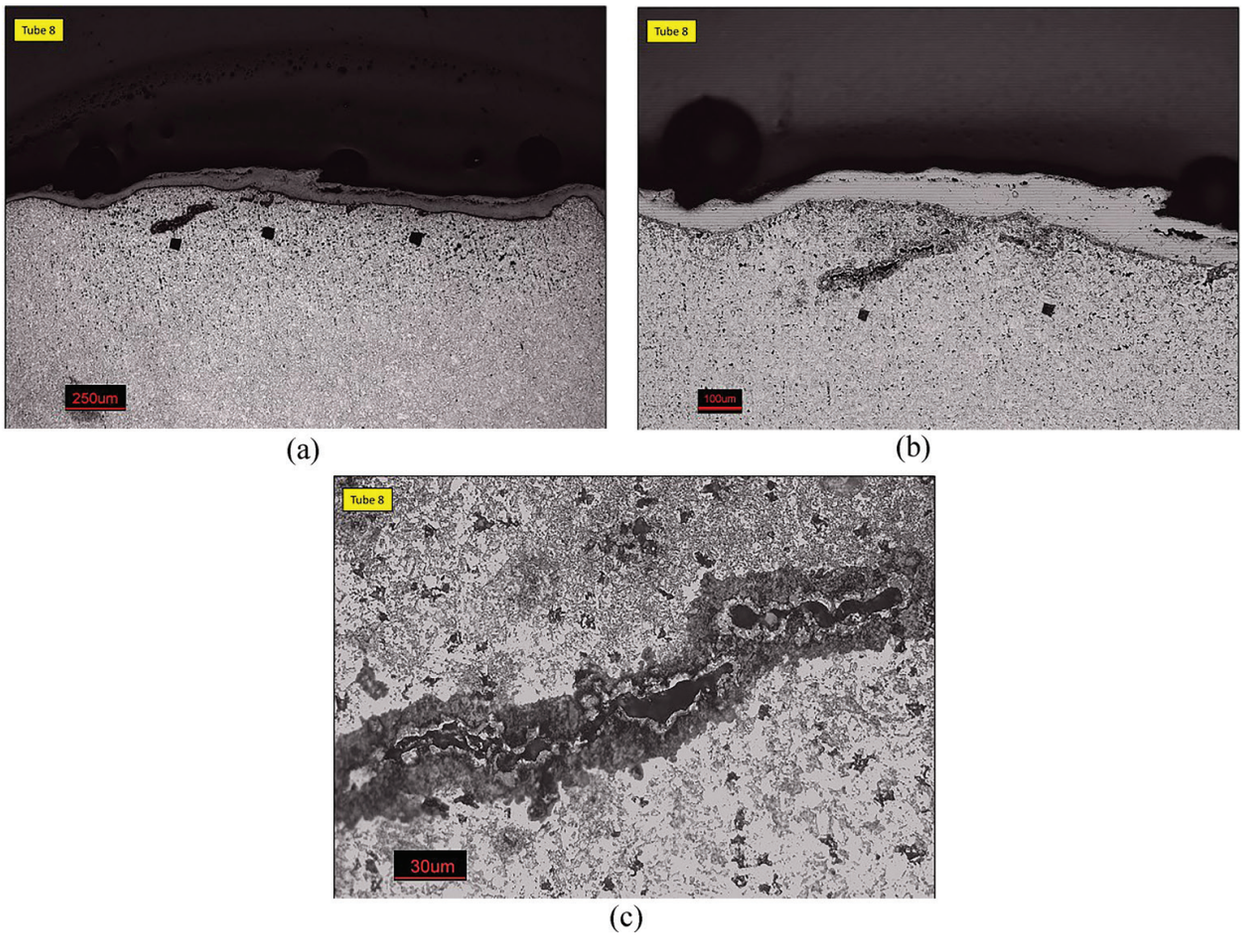

Figure 8. The microstructure of Tube 8 shows a crack at different magnification: (a) 250 μm, (b) 100 μm and (c) 30 μm.

The result of hardness testing is reported in **Table 6**.

Based on the ASTM 213 T91 code, the maximum hardness for tube material 91 is 265 HV [3]. Based on experience, the low alloy material 91 hardness should not be less than 195 HV. The base metal of the tested part was considered still within design specification. The HAZ has a low hardness property, which is considered not acceptable, especially 142 HV, which indicates progressive thermal degradation.

Location	Average hardness (HV)	
	Tube 8	Tube 18
Weld joint	206	267
Heat-affected zone (HAZ)	142	185
Base metal	212	220
Base metal	202	221

Table 6. Average hardness value of selected locations of Tube 8 and Tube 18.

http://dx.doi.org/10.5772/intechopen.72116

3.5. X-ray fluorescence (XRF) analysis

Using a Niton XLt 898 XRF analyser, a positive material identification (PMI) analysis was carried out on the four tube sections (i.e. Tube 8, Tube 9, Tube 10 and Tube 18). Prior to the analysis, the external surface of each section was ground back to bright metal, and the analysis was carried out for three times. For the elements analysed, the average results obtained from both analyses on each section are summarized in **Table 7**, together with the range in composition specified for ASTM A213-09 Grade T91, shown for comparison.

Within the limits of the instrument used, the results of the XRF analysis showed that all four sections were manufactured using ferritic alloy steel, which conformed to Grade T91, that is the specified grade of material. One minor anomaly was the chromium contents of the R3 Tube 18, which contained 7.9% Cr, marginally below the minimum specified chromium content of 8.00%.

3.6. Operational assessment

3.6.1. Statistics of failed/repaired tube

The plant had experienced several HRSG tube failures for its HPHTSH section during its 12 years of operations. Statistics of the tube failures by locations are as per Failure 14, which shows that the majority of the failure has occurred at the right sidewall, followed by the left sidewall. Based on computational fluid dynamic (CFD) study done by third-party consultant (Andreas F., 2015), it was found that there are uneven flow and temperature distribution of the GAS turbine exhaust gas over the HPHTSH section. As shown by the flow study, during the base load operation of 350 MW, the flow is mainly concentrated at the two sidewalls while at the minimum load operation of 210 MW, the flow is channelled only to concentrate at the right-sidewall of the HRSG. Over its 12 years of operations, these operations had caused some tubes for the section to have higher tendency for creep damage as opposed to the others. The failures in the middle section were identified to be related to the acoustic baffle plates, which had been resolved in the past.

From the temperature trending, there are significantly more than six readings where the temperature drops below 100°C within 1-year period. The frequent start-stop, especially cold start, may accelerate thermal fatigue damage, for example, ligament cracking in stud locations (**Figure 9**).

Tube no	Element (wt%)					
	Chromium	**Molybdenum**	**Nickel**	**Manganese**	**Vanadium**	**Niobium**
Tube 8	8.40	1.06	0.11	0.52	0.20	0.08
Tube 9	8.10	0.97	0.07	0.52	0.21	0.08
Tube 10	8.40	1.02	0.06	0.49	0.23	0.08
Tube 18	7.90	0.97	0.10	0.55	0.23	0.08
ASTM A213 Grade T91	8.00/9.50	0.85/1.05	0.40 max	0.30/0.60	0.18/0.25	0.06/0.10

Table 7. The chemical composition of defective tube [3].

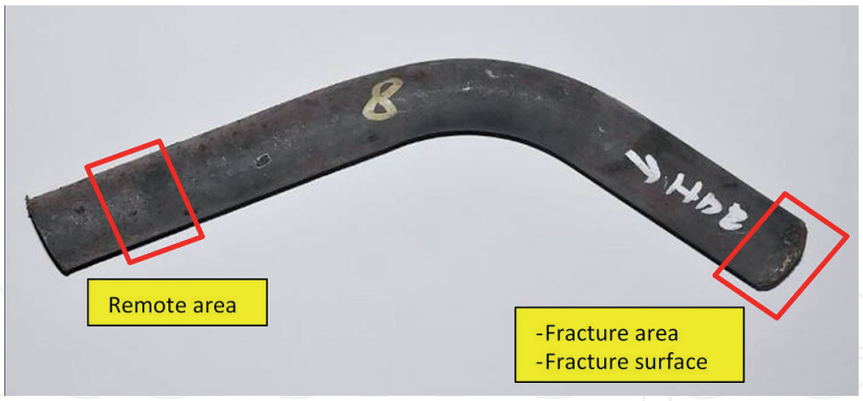

Figure 9. Dimensional reference of oxide thickness measurement.

3.7. Oxide thickness assessment

The location of interest for internal oxide assessment for Tube 8 and Tube 18 is shown in **Figure 9**.

3.8. Comparison

The steam-side oxide scale of micro specimens of Tube 8 and Tube 18 was measured under optical microscope. Both Tube 8 and Tube 18 were found to have undergone excessive steam oxidation. The oxide layer had cracked. The oxide thickness was measured and tabulated in **Figures 10** and **11**. The maximum thickness of the steam side oxide scale was 363 μm for Tube 8 and 390 μm for Tube 18.

Based from steam oxidation calculation [4], the thick oxide scale suggested that both Tube 8 and Tube 18 had been exposed to temperature in excess of 615°C as compared to material specification of SA 213T91 (design temperature, 602°C). The two tubes had experienced long-term overheating during operation.

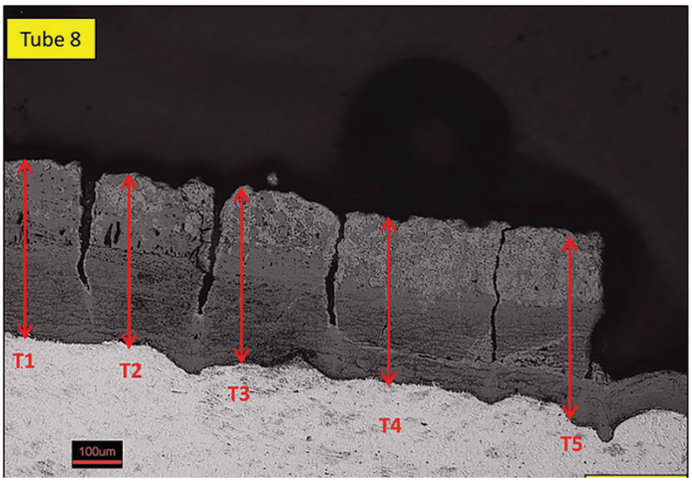

Points	Thickness (μm)
T1	369.44
T2	358.33
T3	361.11
T4	350.00
T5	377.78
Average	363.33

Figure 10. Internal oxide thickness at Tube 8 (fracture area).

http://dx.doi.org/10.5772/intechopen.72116

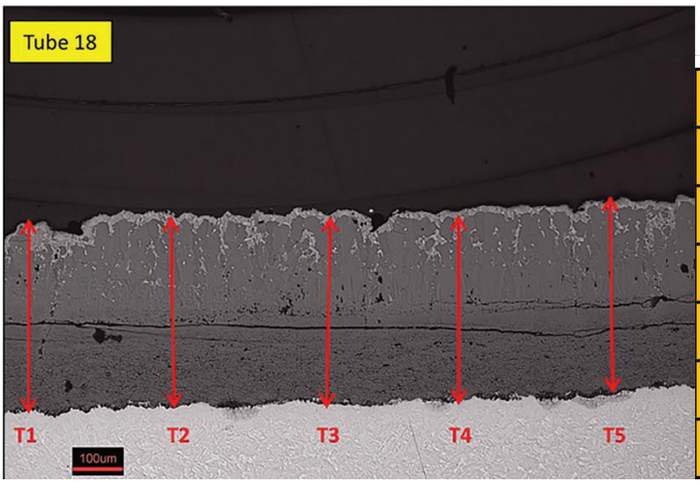

Points	Thickness (μm)
T1	394.44
T2	388.89
T3	388.89
T4	383.33
T5	397.22
Average	390.554

Figure 11. Internal oxide thickness at Tube 18 (remote area).

Tube	Average oxide thickness (μm)	Exposure temperature (°C)	Exposure hour
Tube 8 (internal fracture)	363	630.74	85,000
Tube 8 (internal remote)	270	610.4	85,000
Tube 8 (fracture surface)	118	630.74	8982
Tube 18 (internal fracture)	355	629.18	85,000
Tube 18 (internal remote)	322	622.4	85,000
Tube 18 (fracture surface)	107	629.18	7722

Table 8. The correlation between oxide thickness and exposure temperature/hour using oxide kinetic model.

From the steam oxide calculation, the oxide-filled fracture paths indicated that the cracks had existed for more than 7000 h. **Table 8** shows the oxide calculation based on oxide model.

Both the tubes (i.e. Tube 8 and Tube 18) have been exposed to temperatures of more than 600°C as compared to material specification of SA 213T91, where the design temperature is only 602°C. With this exposure, it had further promoted degradation of tubes material and formation of creep cavities. For fracture surface at Tube 8, with oxide thickness of 118 μm, the crack had been initiated for 8982 h. For fracture surface at Tube 18, with oxide thickness of 107 μm, the crack had been initiated for 7722 h.

3.9. Summary of analysis

The cracking showed the following characteristics:

a. Fairly straight

b. Mainly transgranular

c. No branching

d. Filled with thick oxides

e. Numerous aligned cavities in the vicinity of the cracks

The above observation suggested that the tubes had likely suffered a combination of two damage mechanisms, which were fatigue and short-term creep. The numerous and extensive creep cavities in the HAZ suggested that the tubes at the weld region had undergone advanced and progressive creep damage. For Tube 8, microcracks had formed and the creep damage was classified as 4 according to rating guideline provided in the NORDTEST NT TR 170 (1992) code. For Tube 18, the creep cavities were preferentially oriented and aligned, suitably to be classified as 3.3 according to the NORDTEST rating. The heavy thermal degradation was supported by the low hardness readings at the HAZ (minimum 142 HV was reported, as compared to acceptable range 200 HV–260 HV). It was obvious that the two tubes had undergone time-dependent, high-temperature creep process.

The plant had been operating as peaking plant, and it was subjected to daily start-stop. As the HAZ of the connecting tubes had experienced high-temperature creep degradation after 85,000 h had elapsed, the creep-fatigue cracks could have initiated at this weak region. The propagation was accelerated by the thermal cyclic stress, which was imposed by daily start-stop.

The creep mechanism could have been promoted by the following factors:

a. Defective FCD causing the instability of heat flux distribution, excessive metal temperature, and localized heating at the tubes (HPHTSH header metal temperatures were high, more than 602°C, the T91 limit).

b. Poor quality of HAZ (possibly caused by improper PWHT).

The thermal fatigue could have been promoted by thermal stress imposed by daily start-stop cycles.

4. Conclusions and recommendations

The cracks at the HAZ of the Row 3 connecting tubes at HPHTSH header could be attributed to creep-fatigue damage. The following contributory factors were identified:

1. Excessive metal temperature, as compared to design value.

2. Low hardness property at HAZ (creep strength was low).

3. Long service exposed hours (85,000 h–approaching 100,000 h).

4. Frequent start-stop cycles.

5. Localized heating due to instable heat flux distribution (contribute to creep)

Nevertheless, the remaining wall thickness had reduced to less than the minimum required thickness of 2.8 mm; the tubes were prone to stress-rupture failure, which might have occurred in short term. Some of the recommendations are given as follows:

1. As the connecting tubes had begun to show signs of advanced creep damage at HAZ, there is likelihood that the header, especially at the weld and HAZ had also undergone similar creep damage. It is recommended to conduct extensive replication and hardness testing at all the connecting tubes and header shell during outage opportunities. The area of interest is weld and HAZ.
2. The thickness profile of all the affected superheater tubes shall be measured in extensive manner during outage opportunities. Tube sections with remaining wall lower than minimum required thickness shall be cut and replaced.
3. As the plant is subjected to daily start-stop recently, it was recommended to conduct borescope inspection inside header to check for ligament cracking. It was also proposed to minimize the request from the single buyer in order to minimize the daily start/stop, thus, minimizing the cyclic operation and fatigue stress.
4. The plant should consider on conducting a comprehensive life assessment study on the boiler, as the service hours had approached 100,000 h and signs of creep damage had emerged.

Author details

Ainul Akmar Mokhtar*† and Muhammad Kamil Kamarul Bahrin†

*Address all correspondence to: ainulakmar_mokhtar@utp.edu.my

Universiti Teknologi PETRONAS, Perak, Malaysia

† These authors contributed equally.

References

[1] ASM International. Introduction to Steels and Cast Irons—Metallographer's Guide: Irons and Steels. Ohio: ASM International; 2002

[2] ASME. Section V – Non-Destructive Examination. ASME Boiler & Pressure Vessel Code. New York, NY: The American Society of Mechanical Engineers; 2015

[3] ASME. Section II Part D–Material Properties. ASME Boiler & Pressure Vessel Code. New York, NY: The American Society of Mechanical Engineers; 2015

[4] API Std 579-1/ASME FFS-1. Fitness-For-Service. Washington, DC: American Petroleum Institute; 2016

IntechOpen